MINISTÉRIO DA CIÊNCIA E TECNOLOGIA
INSTITUTO NACIONAL DE PESQUISAS ESPACIAIS

INPE-15216-PRE/10078

NEW FUEL CELL ARCHITECTURES AND THE ROLE OF ELECTROKINETIC FLOWS IN ITS PERFORMANCE

Luis Antonio Waack Bambace
Fernando Manuel Ramos
Hélcio Francisco Villanova
Alfredo José Alvim de Castro*
Renata Cristina Favalli*

* IPEN

INPE
São José dos Campos
2008

Publicado por: **esta página é responsabilidade do SID**

Instituto Nacional de Pesquisas Espaciais (INPE)
Gabinete do Diretor – (GB)
Serviço de Informação e Documentação (SID)
Caixa Postal 515 – CEP 12.245-970
São José dos Campos – SP – Brasil
Tel.: (012) 3945-6911
Fax: (012) 3945-6919
E-mail: pubtc@sid.inpe.br

Solicita-se intercâmbio
We ask for exchange

MINISTÉRIO DA CIÊNCIA E TECNOLOGIA
INSTITUTO NACIONAL DE PESQUISAS ESPACIAIS

INPE-15216-PRE/10078

NEW FUEL CELL ARCHITECTURES AND THE ROLE OF ELECTROKINETIC FLOWS IN ITS PERFORMANCE

Luis Antonio Waack Bambace
Fernando Manuel Ramos
Hélcio Francisco Villanova
Alfredo José Alvim de Castro*
Renata Cristina Favalli*

* IPEN

INPE
São José dos Campos
2008

New Fuel Cell Architectures and the Role of Electrokinetic Flows in its Performance

L.A.W. Bambace, *INPE*, F.M. Ramos, *INPE*, H.F. Villanova, *INPE*, A.J. Alvim de Castro, *IPEN*, R.C. Favalli, *IPEN*

***Abstract*--This papers discusses the role of: transport phenomena, electrokinetic flows, gas-liquid interface area, convective mix, and the electrical boundary layer (EBL) in fuel cell performance. The electrokinetic phenomena analysis is based in a new model of electrocapillary flow, and its preliminary experimental tests. With this model, oxygen transport and convective ionic current in high specific area electrodes are analyzed. The paper also shows the use of the Critical Chain Method (CCM) in the appraisal of feasibility, costs and risks of innovative fuel cell set ups.**

***Index Terms*-- Fuel cells, Fluid flow, Boundary Layers, Electrochemical devices, Electrochemical processes;**

I. Nomenclature

A	- surface area
$[a_i]$	- concentration of dissolved ion i
a_∞	- bulk ion concentration
B_i	- influence coefficient
b_k	- constants in Grahame formula
C	- electrical capacity
c	- capacity per area
c_m	- capacity per area of dEBL
c_2	- capacitance per area of nEBL
EBL	- electric boundary layer
$\mathbf{E}_o$	- Surface parallel electrical field
EKF	- electrokinetic flow
EOF	- electroosmotic flow
dEBL	- diffuse electric boundary layer
D_i	- diffusion coefficient
$\mathbf{E}_x$	- Surface normal electrical field
F	- Faraday constant
h	- slip factor
K	- Inverse of Debyer length
nEBL	- non-diffuse electric boundary layer
P	- Pressure
P_∞	- Pressure far from surface
PB	- Poisson-Boltzmann
PEM	- Proton Exchange Membrane
R	- Universal gas constant
U	- electrical potential
U_w	- wall electrical potential
u	- fluid velocity
u_m	- speed profile component
u_p	- electroosmotic speed component
v_p	- electrocapillary speed component
v_{OHP}	- nEBL slip speed
x	- normal coordinate
z	- number of charges of an ion
α	- accommodation coefficient
δ	- conversion factor
ε	- media dielectric constant
ϕ_w	- fluid potential less U_w
γ_e	- volume charge density
φ	- non-dimensional potential
μ	- dynamic viscosity
ρ	- ionic resistivity
σ	- surface tension
σ_o	- pure liquid surface tension
ω	- fluid density
ζ	- potential inside EBL

II. Introduction

Each low temperature fuel cell has different transport phenomena restrictions. Standard plane gas-liquid interface PEM flooded models show that its peak power O_2 entry by diffusion is limited to a few nanometers [1]. The use of test probes inside such PEM electrodes proved that only a tiny part of the catalyst layer is truly active [13]. PEM set ups with catalyst in its diffuser carbon filaments have no vital O_2 transport limits, but strong ionic current drain. The Adams-Watson-Bacon fuel cell had, beside the problem of low O_2 solubility in alkaline liquids [2], great ionic current restrictions due to its electrodes low electrolyte volume fraction, air channels and particle scales tortuosities [11]. Ledoux et al. [3] used carbon fiber with covers of entangled carbon nanotubes as fuel cell electrodes. Bambace et al. [6,15,16] used tubular setups. MEMS based and micro-fluidic fuel cells and other non standard setups are also in the literature [5,6,12]. Such new setups have many Degrees of Freedom (DOF) that affect their operation, and we need to understand all effects to evaluate the potential advantages of such systems. In electroosmotic flow (EOF) chemical reactions control charge levels in the EBL as dissociation of surface silanol or PEM membranes sulfonic groups. Capacitive effects prevail in electrocapillary systems (metal-bath interfaces). Top speeds in 1-10 μm metal ducts can´t be found with a simple capillary and pressure drop forces balances: the flow itself reduces its force drivers, as in thermocapillary flow. The Knudsen number (Kn) based on EBL thickness is 0.03-0.15, so Kn might be in the slip flow range. Surface diffusion and the mobility of adsorbed ions are known to reduce the roughness of electroplated parts. So, the non-slip condition is not valid, and experiments are needed to obtain new flow models. Convective mixing may appear in some cases due either to Bénard cells or tortuous flows induced by random nanometer features.

L.A.W. Bambace , F.M. Ramos, and H.F. Villanova are at INPE- National Institute for Space Research PO Box 515 São José dos Campos, BR (e-mail bambace@dem.inpe.br, fernando@lac.inpe.br, hnova@lac.inpe.br)

A.J. Alvim de Castro and R.C. Favalli are at IPEN – Institute of Nuclear and Energy Research, Av. Lineu Prestes. 2242, São Paulo, BR (e-mail ajcastro@ipen.br renata.favalli@gmail.com)

Convection helps ionic current transport only if the electrolyte is not neutral, i.e., inside the EBL, which is thin to reduce electrical potential energy. Onsager´s principle [7] implies that an electrokinetic flow (EKF) only appears if it reduces the system entropy generation. So the power required to keep EKFs comes from a fall in another kind of dissipation. There are difficulties in achieving reliable and repetitive building processes of new setups. So, feasibility and risks of innovative projects was studied with a version of the Critical Chain Method that can rank research options, not only hinting the need of doing any option, but saying when to start it, based on the outputs of already scheduled activities.

III. Models Description

Static electrocapillary was described in the 19th century by Lippmann, who noticed that mercury surface tension had a parabolic profile with a maximum for uncharged liquid. For molecules with dipoles in the electrolyte, the surface tension σ is given by:

$$\sigma = \sigma_o - 0{,}5\ (C/A)\ \Delta U^2 + \ \Sigma_{i\{}\ B_i \ln(1+ b_k\ [a_i])\ \}\qquad (1)$$

where σ_o is the uncharged pure liquid surface tension, C the electrical capacity, A the area, U the electrical potential, $B_i \in R$, an influence coefficient, $[a_i]$ the concentration of dissolved ion i, and b_k are constants. The energy is the dσ/dx integral over a surface, so capillary force in any channel of fixed perimeter p, with tip σ values being σ_1 and σ_2 and $p\,(\sigma_1-\sigma_2)$. For a tube of diameter d, length L, and fluid dynamic viscosity μ, the force balance is given by the flow speed of $(\sigma_1-\sigma_2)\,L^{-1}\mu^{-1}d/8$ if standard speed profiles are used. Large tubes don´t show such speeds no matter what causes the changes of σ. An EBL of thickness x_o has a non-diffuse part of thickness x_2 (nEBL) of organized layers over adsorbed anions and molecules where dipoles forces prevail. It also has a diffuse sublayer (dEBL) that obeys an one-dimensional Gauss equation, as Poisson-Boltzmann (PB) so for $\varphi = U\,F/(R\,T)$, and q=1:

$$\nabla^2\varphi = \varepsilon^{-1}\ \gamma_e = -\ K^2\,\Sigma\ n_i\ n_o^{-1}\ \exp(-q\ z_i\varphi)\qquad (2)$$

where the potential reference is set far away from the surface, a place with ion concentration a_∞, F is the Faraday constant, R the universal gas constant, T the absolute temperature, K is $[2z_i^2F^2a_\infty(y)]^{1/2}[\varepsilon\,R\,T]^{-1/2}$ for y a coordinate parallel to the surface, z_i the number of charges of ions, γ_e the volume charge density, ε the media dielectric constant. Replacing Boltzmann distribution other equations arise [8-9], generally written in similar form with other q and K, at least as an approximation. The solution of equation (2) is often written for constant $z_i=z$ in implicit form:

$$\tanh(0.25\ \varphi) = \tanh(0.25\ \varphi_{2(y)})\ \exp(-K\ (x-x_2))\qquad (3)$$

where $\varphi_2(y)$ is the dimensionless potential at x_2, and x the distance from the surface. Equation (3) may be rewritten, with help of $\delta = z\,F/(R\,T)$ and $\zeta(y)=\varphi_2(y)\delta^{-1}$ in explicit form as:

$$G(x,y)= \tanh(0.25\ \delta\ \zeta_{(y)})\ \exp(-K\ (x-x_2))\qquad (4.a)$$

$$U(x,y)= 2\ \delta^{-1}\ \ln\{1+G(x,y)\}\ -\ 2\ \delta^{-1}\ \ln\{1-G(x,y)\}\qquad (4.b)$$

Unit area capacities $c \equiv (C/A)$ may be split in diffuse and non-diffuse parts, $c_m=(x_o-x_2)/\varepsilon$ and $c_2=x_2/\varepsilon$. PB fails to model cathode and anode c differences. In the EBL there is an electrical field $\mathbf{E}_o$ in the direction $\hat{\mathbf{e}}_y$ and a much stronger field $\mathbf{E}_x$ in the direction $\hat{\mathbf{e}}_x$ normal to the metal surface, where charge density ν is $[8\,RT\varepsilon\,a_\infty]^{1/2}\sinh(0.5\,\delta\zeta)$ in PB. U and ionic resistivity ρ obeys the Laplace Equation, thus for E the electrical field:

$$c^{-1} = \{\varepsilon^{-1}\,[\cosh(\delta\,\zeta(y)/2)]^{-1}\,K^{-1}+\varepsilon^{-1}x_2\}\ = c_2^{-1}+c_m^{-1}\qquad (5)$$

$$\mathbf{E} = -\nabla U\qquad (6)$$

$$\nabla\rho^{-1}\nabla U = 0\qquad (7)$$

As the layer is thin $\gamma_e \sim \varepsilon\ d^2U/dx^2$. Continuity, Navier Stokes and species concentration equations are:

$$\nabla\cdot\mathbf{u} = \nabla\cdot(u_x\ \hat{\mathbf{e}}_x + u_y\ \hat{\mathbf{e}}_y) = 0\qquad (8)$$

$$\omega\ u_i\ d\mathbf{u}/dx_i = -\nabla\ P + \mu\nabla^2\mathbf{u} + \gamma_e\ \mathbf{E}\qquad (9)$$

$$-D_i\ \nabla^2 a_i + \mathbf{m}_i\ \nabla\cdot(\mathbf{E}\ a_i) + \nabla\cdot(\mathbf{u}\ a_i) + \chi_{qi} - \chi_{qo} = 0\qquad (10)$$

where ω is the fluid density, a_i species i concentration, χ_q and χ_φ chemical conversion rates, $\mathbf{m}_i$ ionic mobility, D_i diffusion coefficient. EBL speed component normal to a solid is negligible, and, 2 nm<x_o<5 nm, to P_∞ the far away pressure, pressure is $P(x,y)=P_\infty(y)+\varepsilon\,(dU/dx)^2/2$. Due to adsorbed ions surface diffusion and mobility of, and a possible slipping boundary condition, a tube fluid velocity **u** may be split in 4 wall parallel parts: a nEBL slip v_{OHP} at x_2, $u_p=(\zeta-U)\varepsilon\,\mathbf{E}_o\mu^{-1}$, $u_m=U_m(r^2/R^2)$, and v_p; and **s** normal to wall. G≡0 out of EBL, dU/dx=0 if U=0, so:

$$[\varepsilon\ d^2U/dx^2\mathbf{E}_o-\mu d^2u_p/dx^2]+$$
$$+[dP/dy+4\mu U_m R^{-2}+\Delta\ P_a+\omega u\ du/dy\ +\omega\ s\ du/dx]\ -$$
$$-[\mu d^2v_p/dx^2-\varepsilon\ dU/dx\ d^2U/dxdy-\varepsilon\ dU/dy\ d^2U/dx^2]\qquad (11)$$

Setting the 1st line of equation (11) to zero, one gets the classical EOF equation, solved by the u_p, the 2nd line governs flow out of the EBL, and is solved by u_m if **s**≡0. The 3rd bracket refers to the electrocapillary extra component v_p, function of electrical variables only. For $x-x_2<x_o-x_2$ and $L=2\,\mu^{-1}\varepsilon\,\delta^{-2}\,a_\infty^{-1}da_\infty/dy$:

$$dv_p/dx = \mu^{-1}\varepsilon\,dU/dydU/dx\qquad (12)$$

$$Y = -\ 2\ \mu^{-1}\varepsilon\,\delta^{-1}\,\mathrm{cosech}(\delta\zeta/2)\,(d\zeta/dy)\qquad (13)$$

$$v_p = [1-G(x,y)^2]^{-1}\,\{Y-L\,K\,(x-x_2)\}+$$
$$+\,L\ln[(1+G(x,y))/(1-G(x,y))]\tanh(\delta\zeta/4)^{-1}\qquad (14)$$

See that a_i and a_∞ vary in finite gaps due to dissociation changes that overcome migration of non-reacting ions. For 2D cases with a fixed wall potential U_w, $\phi_w \equiv U_w-U$ is the total EBL cross potential, at $\phi_w = 0$, $d\phi_w/dy=(x_2\ K+1)\ d\zeta/dy$, so for linear U profile outside a PB EBL, with K and capacitance definitions, it is possible to write:

$$d\phi_w/dy = -0.5\,(U_w-\zeta)\ a_\infty^{-1}da_\infty/dy$$
$$-0.5\,\delta U_w[\tanh(\delta\zeta/2)]^{-1}d\zeta/dy+0.5\,\delta\zeta\tanh(\delta\zeta/2)d\zeta/dy\qquad (15)$$

The integral of $\gamma_e(u_p+u_m+v_p+v_{OHP})$ in the $\hat{\mathbf{e}}_x\hat{\mathbf{e}}_z$ planes is the flow current. As dEBL is thicker for low ϕ_w the peak u_p+v_p is in low ϕ_w zone, where flow current is minimal. Ignoring EBL area in mass balance $U_m(y)=\ddot{U}_m-\Sigma\{v_{p\infty}(y)+u_{p\infty}(y)+v_{OHP\infty}(y)\}/2$, and integrating 2nd line of equation (11) for given tube end pressures, one gets $\ddot{U}_m$. For tubes of 10^{-5} m, U profile is near linear, to 10^{-8} m systems, flow current is high and this ionic potential drop outside EBL is nonlinear, so iterative schemes and $\hat{\mathbf{e}}_y$ interpolation are used to find dU/dy. Equation (7) is solved only inside EBL, and out of it real profile approximated with straight line segments, as for each grid element current is assumed constant. v_{OHP} minimizes the sum of plastic all dissipations, including the nEBL plastic one if ϕ_w is high. For EBL thickness with small face grid scales, it is wise to supply the total EBL slip to the CFD model as a function of local ϕ_w. In general electrode potentials, total current and chemical kinetic models the are known. EKF test set ups have one channel and connected metal surfaces in short circuit, so the ϕ_w profiles minimize capacitive energy. Reactions may occur in insulated metallic parts, as tips work either as a secondary cathode or anode if

$d\phi_w/dy$ is high. For **n** molecules by unit of volume with mean cross section diameter ξ, the mean free path λ is $(2^{0.5}\pi n\xi)^{-1}$. Reference [10] hints a slip $(2-\alpha)\mu^{-1}\alpha^{-1}\lambda\tau_x+.75(\gamma-1)\gamma^{-1}\mu\omega^{-1}T^{-1}dT/dx$. Its dT/dx part ($\psi$) is the thermocapillary slip, τ_x is the hydrodynamic stress $\mu du_m/dx$, α and γ accommodation coefficients. For high ϕ_w, x_o-x_2 and ζ vanish. So with this slip as example we took $v_{OHP}=(2-\alpha)\mu^{-1}\alpha^{-1}[\mu\lambda du/dx+\mathbf{h}\varepsilon c\phi_w E_o]$, with **h**=0 for $\phi_w<\phi_c$, with nEBL yield strength reached at ϕ_c. EBL forces may bias the molecules shifts due to thermal shocks. Thus, it may happen that **h**≠0 always, v_p and u_p may be high in some points, but cathodic and anodic values are opposed to each other, and don't explain EKF flow for asymmetric ϕ_w fields. Equation (14) is not true at ϕ_w=0, where a wall outward wall flow can´t be ignored, s≠0. v_p and v_{OHP} main driver is pressure change, there is an electrostatic pressure due to charge unbalance in EBL. Without dEBL, it is easy to see that the nEBL pressure gradient times its thickness is exactly the electrocapillary force. The total pressure force in the EBL is always equal to the electrocapillary force, although it is not so easy to prove. Multiplying ψ by $u\omega d\mu^{-1}$, it´s easy to see that ψ is a speed.

IV. Experimental Verification

The theoretical model and an α=1 hypothesis were tested with the setup showed in Figure 1. Electroplating tapes were placed to avoid unpredicted passages due to distortion of PVC parts. The potential difference cross the 2 pools gives passages ionic current. Applied current was measured directly. Both currents are equal if applied potential is less than twice the electrolysis one, if not metal channel metallic annexes work either as a secondary anode or cathode. Ionic resistivity ρ was found with fixed current, i, and 2 smooth gold plates of area S in a rectangular box. Moving a plate, only the current path L changes, so steady state applied potential change is $i\rho\Delta L/S$. The rest of applied potential is due to activation and boundary layer polarizations (see figure 2). All parts were jointly electroplated, with distinct cathode current controls. Due to some degree of porosity and corrosion, it was not possible to do alkaline tests, or to replace the tape barrier by more regular one. Acid tests were filmed with applied potential at main electrodes from 1.4 to 3.2 V, in 0.2 V steps. Bubbles hit one another in the channel and join themselves in bigger ones, as well as arrive at the fluid upper surface, or hit the walls. In 63 s films, 3 to 5 bubbles that pass directly through the entire channel were found. Events were observed frame by frame with the VirtualDub software, to obtain the average bubble speeds in the channel to each applied potential. The selected frames were exported to JPEG format with this program. Figure 3 shows 5 frames took from one of the films that shows a bubble passing the channel. Average speeds are proportional to average surface tension force. As the capacitive energy of channel and surrounding metal parts is minimal, and as anodic zone has a limit capacitance of 0.2 F/m^2, and cathodic zone a 0.7 F/m^2 one, channel tip potentials were found to be at a rate of 0.37 in modulus. Total channel potential were measured with Pt 36 AWG wires. With this we found an **h** value of 57±15. Errors come from oxidation, bad cleaning, corrosion rate and errors in electrical measurements, as nEBL thickness of clean surfaces are less than 0.3 nm. Cleaning is decisive to EKF intensity level.

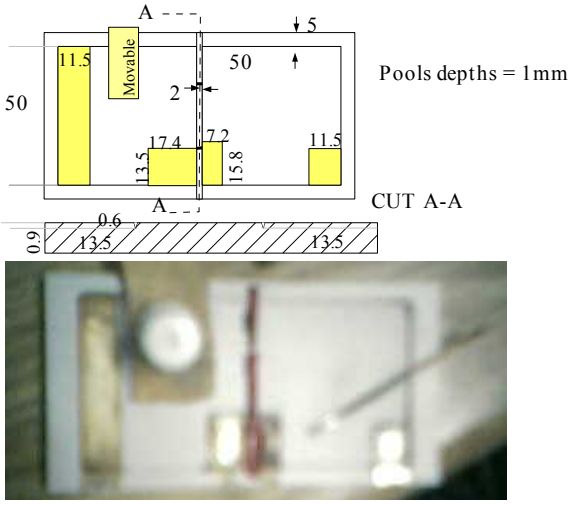

Fig 1: Flow test Arrangement.

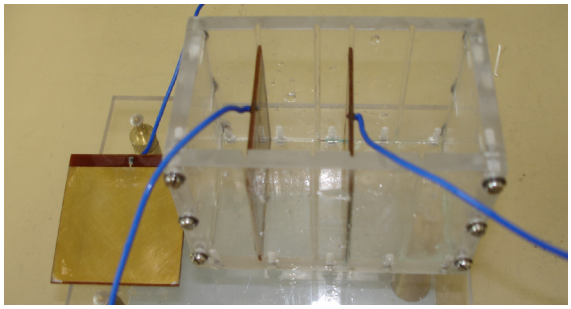

Figure 2: Ionic conductivity test set up.

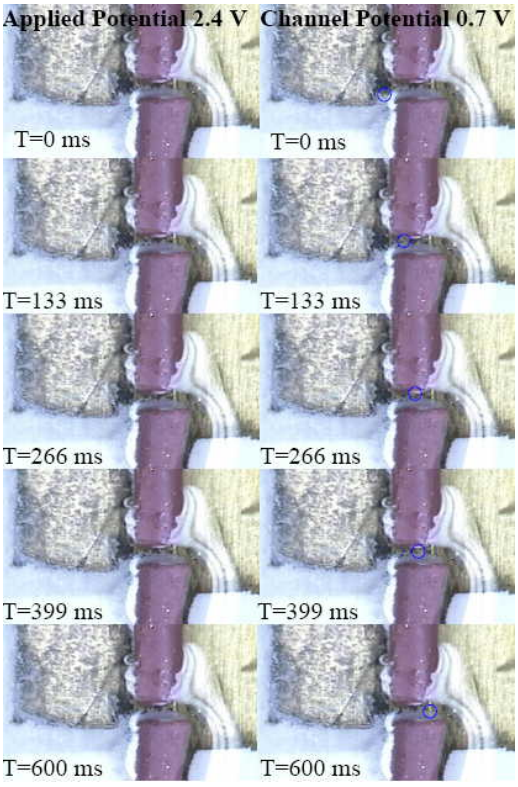

Fig. 3 Bubble flow in a very clean metallic channel

TABLE 1: SUMMARY OF MAIN TEST DATA FOR H_2SO_4 SOLUTION.

Total Potential (V)	**Channel Potential** (mV)	**Current** (mA)
1.40	166	1.15±0.15
1.60	371	3.5±0.3
1.80	563	12.5±0.3
2.00	754	18.4±0.3
2.20	959	22.3±0.3
2.40	1.21	29.3±0.2
2.60	1.32	36.7±0.3
2.80	1.57	42.3±0.1
3.00	1.76	50.0±0.1
3.20	1.87	57.8±0.3

TABLE 2: FLOW CURRENT DATA FOR NI M-TUBES WITH 6 M KOH.

Applied Potential (V)	**Total Lenght** (mm)	**Null ϕ_w Point** (mm)	**Peak Flow Current** (μA)	**Meam Bulk Current** (μA)
0.1	0.80	0.10	0.0487	0.0188
0.2	0.80	0.10	0.383	0.0377
0.3	0.80	0.10	1.29	0.0565
0.4	0.80	0.10	3.07	0.0754
0.1	0.80	0.40	0.0335*	0.0188
0.2	0.80	0.40	0.224	0.0377
0.3	0.80	0.40	0.755	0.0565
0.4	0.80	0.40	1.79	0.0754

V. NUMERICAL RESULTS

A common Pt catalyst membrane painted PEM was studied with the flooded model to generate a baseline solution. It has a very weak EKF, as contact resistances and ionomer insulation limits ϕ_w to small values. Later, we studied the fuel cells of Figures 8 to 11: the Bacon cell, the Ledoux carbon nm-tube and fiber plies PEM, and 2 μ-tube cells. In these 4 cells, the gas goes from a high pressure to a low pressure zone, passing through the pores or through a 3 mm thick non-woven arrangement of tubes or coated plies, separated by large pore foams with end thickness of 0.2 and 0.8 mm. Preliminary theoretical results for flow current in non-reacting Ni μ-tubes with nm-foam walls, with the acid **h** value instead of alkaline are in table 2. Figures 12-16 give theoretical results for: output potential, efficiency and power for each current without[a] or with[b] EKF. The exchange current for the Ni tubular cell, Figure 14, was $3 \cdot 10^{-5}$ A/m^2, 35% in volume of carded tubes of 5 and 7 μm radius, 100 nm foam texture with 85% of void. PtO_2 reduction exchange current is 0.07 A/m^2. For * marked case, dEBL gives 28% of flow current. CFD analysis predicted 6 to 9 Bénard cells for the arrangements of Figures 9-11, with fibers normal to ionic insulation. The strong flow out of the wall near the ionic zero is an inducer of such cells with lengths ranging from 30 to 150 μm. It shall be seen that even without EKF, performances of cylindrical gas-liquid interface cells are higher.

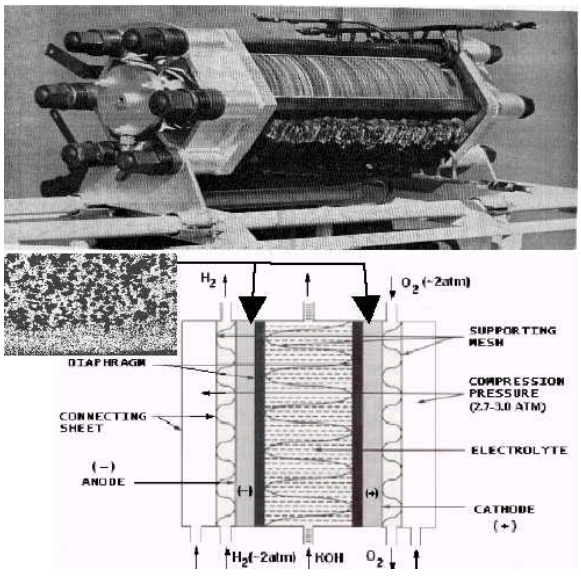

Figure 8: Adams-Bacon-Watson Alkaline Fuel Cell.

CFD analysis predicted 6 to 9 Bénard cells in figures 9-11 set ups, for fibers normal to ionic insulation. The strong flow outward the wall near the ionic zero induces of such cells with lengths ranging from 30 to 150 mm.

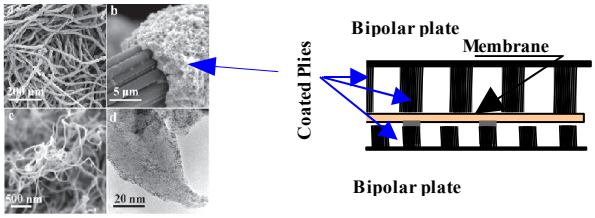

Fig. 9: Ledoux PEM Fuel Cell.

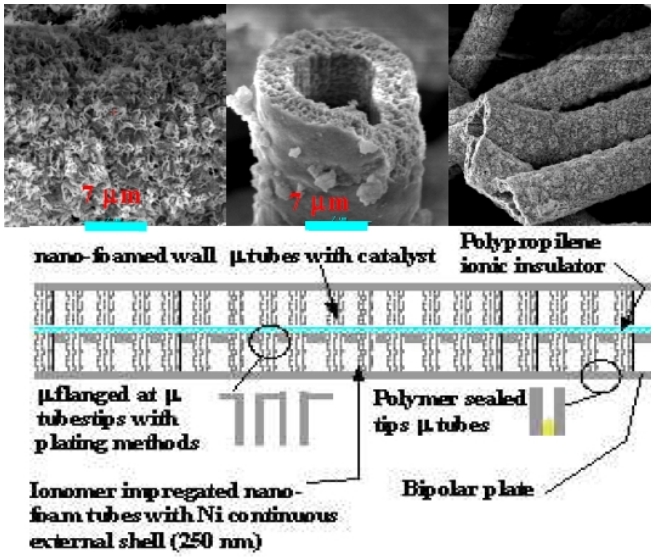

Fig. 10: Nickel nanofoam wall μ-tubes AFC.

The results for cells in Figures 9 and 11depend strongly on the density of the nanotube electric connections and related resistance. It will be seen that even without EKF, performances of cylindrical gas-liquid interface cells are better. Flow current is the major cause for better results of all cells of figures 8 to 11 when they are clean and EKF is present. Tubular cells have better ionic transport, and Bénard cells that slightly enriches their tube cores with O_2, creating a 2nd diffusion path and about 2% more O_2 flux. The foamed tubular cell has random foam surfaces, forcing zig-zag flow, enhancing O_2 transport in 10%, approximately; its current is smaller than Ledoux and tubular acid cells, due to the low O_2 solubility in alkali, but it is a cheaper device. The expenses with noble metal catalyst are the major part of an acid fuel cell cost. Acid corrosion resistance of the cell presented in Figure 10 covered with NiCrN as Los Alamos metal bipolar plates is a doubt.

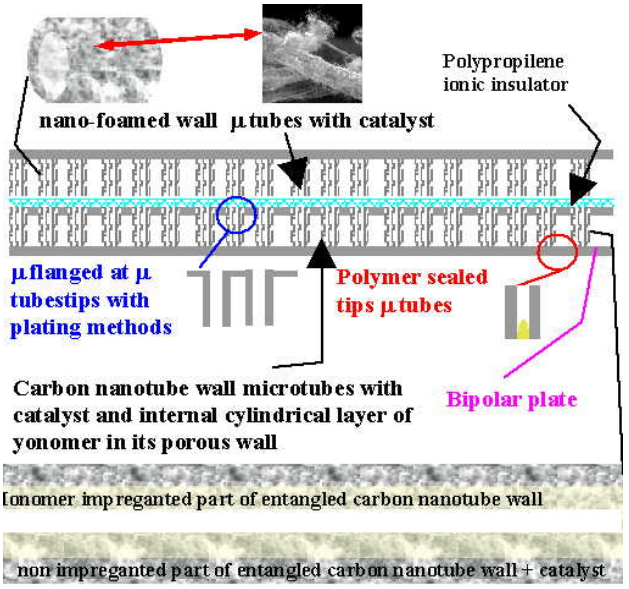

Fig. 11: Carbon nanotube wool wall m-tubes fuel cell.

Cell performance curves were based on chemical kinetic models and on energy conservation, so output voltages are the open cell less the integral of all losses, divided by the currents. O_2 and H_2 local concentration, catalyst data and diffusion flux limits were used to calculate local reaction rates and output currents. Total tubes area is 4 times their actual volume over their diameter. The cell in Figure 11 has more breathing area and available section to ionic conduction than the Ledoux cell and no membrane so its results are better, despite of no flow current in the anode. The cell of Reference [11] has porous carbon tubes with gas inside, catalyst and Nafion outer coats, and tubes are in an electrolyte pool, having power over 8 W/cm^3, despite of its tubes separation. O_2 overpotential η is $RT \ln\{j^2 [a_o]^{-2} 4FD_{eff} i_o \kappa\}/(4F\alpha)$, where j is the current per unit area of the gas-liquid interface, $[a_o]$ the reference O_2 chemical activity, F the faraday constant, D_{eff} the effective diffusion coefficient of porous media, R universal gas constant, T the absolute temperature, i_o the exchange current, κ the area density, α the transfer coefficient. Common PEM cells main loss source is η, and η falls drastically in large area systems of small j. PEM electrodes have also large electrical resistance due to contact resistance between carbon black particles and meaningful membrane ionic resistance. Cylindrical geometries replace exponential solution by an alike eigenvalue I_o Bessel function. Uniform reaction rate tubes have an effective resistance proportional to 1/3 of its length, and real length loss is smaller as reaction rates drops as the distance from ionic bridge rises.

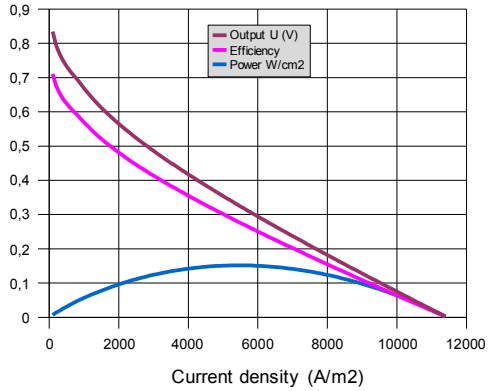

Fig. 12: Simple coated membrane cell performance.

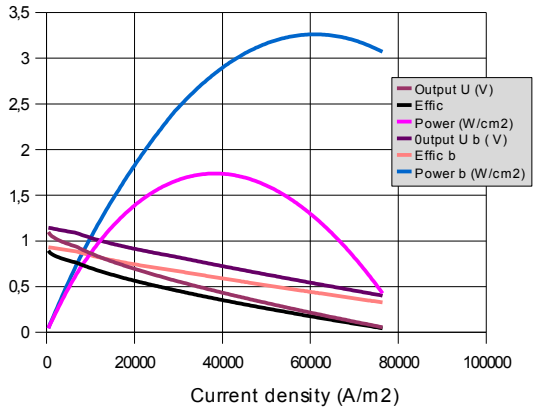

Fig. 13: Ledoux cell performance

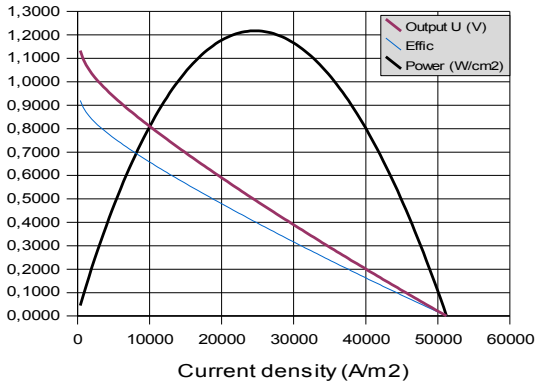

Fig. 14: Adams-Bacon-Watson AFC performance.

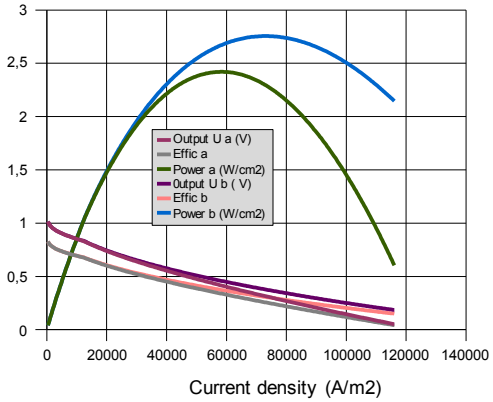

Fig. 15: Nickel nanofoam tubular cell performance.

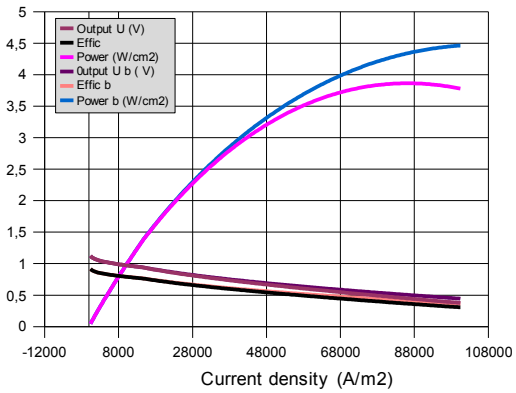

Fig. 16: Nanotube wool wall tubular cell performance.

VI. CRITICAL CHAIN METHOD IN PLANNING

The amount of research on fuel cell research is huge and most efforts are made without any coordination. This policy directs undue efforts to some fields, with many people doing nearly the same work, with lack of assets on other areas. This issue is less crucial in rich than in developing countries. All research projects hava risks. People may not reach desired goals, or a poor quality product may be developed. Research has lots to do with gambling, and good gamblers consider game trees. The delivery of very innovative products in military bids on time, assuring strategic advantages, requires more management expertise than the use of game trees or PERT schemes can provide. The Critical Chain Method (CCM) [14] may be improved with risk control tools employing parallel developments, if needed, judicious decisions about starting or not any extra task, and schedule [16], leading to CCM*. To control a risk, people must know that it exists, so brain storming shall be used to enlist possible troubles and to avoid failures in risk detection. Also the larger the number options studied, the greater the chance to work on a real good one. Fuel cell projects require choices of: geometry, catalysts, materials, gas-liquid interface control, ionic and electrical insulators, as well as fuel and oxidant sealing, separation and supply. Real task trees are too big to detail here, as single subsystems involve many choices. To explain CCM*, system level trees are given in figures 18-20, where rectangles, losangles and circles, match tasks, baffles and decisions listed in Tables 3-5. Failure Risk (**FR)** and Task Duration (**TD)** in weeks, are in the same tables. Comparing tables 3 and 5 for PEMFc systems it is seen that the main success factor is a good detailing of options and risks, which is crucial to innovation and market advantage. The risks of project failure for tubular cells and PEMFC are similar, and differences may be either associated with trees detailing or a real warning of more difficulties. But a tubular cell development needs much more effort and money, the cost of a bigger chance of innovations and a big market in crucial economic sectors. The improvement of techniques is difficult. For instance, to apply common 4-6 nm Pt particles of over any substrate is a low risk task, but there's a lot of risk of not applying 2 nm size Pt particles. Decision in CCM* gets the standard treatment given in CCM for external constraints.

TABLE 3: NO CHOICE TASKS CHAIN FOR MEMBRANE COATED PEM

#	Task / **Decision**	**FR**	**TD**
1	Making a new membrane	0.30	18
2	Developing a system to apply smaller Pt grains	0.30	16
3	Buy bipolar separator, diffuser and faulting parts	0	3
4	Integrate the cell	0.02	1
5	Test thecell	0	3

#	Weeks	#	Weeks	#
1	2	2	2	13

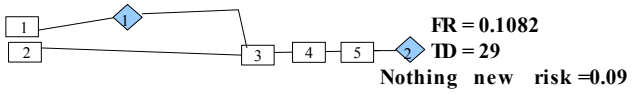

Fig. 18: No choice PEM developing program

Initial studies showed that less active organometalic catalysts may be used due to better O_2 entry. Some of these catalysts stop making four O_2 electrons reduction at high polarization. A more active catalyst in H_2O_2 reduction may be used in the inner part of the tube wall to take advantage of convection. The lack of Pt free acid catalysts data is the main difficulty for the simulation of such designs. The wall total force equals electrical forces in steady state boundary layers, pressure field distributes and relieves the loads, but good quality control is needed to avoid Ni tubes fatigue.

TABLE 4: TUBULAR FUEL CELL TASKS CHAIN.

#	Task / **Decision**/doubt *=>ok	**FR**	**TD**
1	Making Ni nanofoam wall μ-tubes mec. resistance	0.05	16
2	Cr covering of task 1 μ-tubes cover uniformity	0.10	12
3	Nitretation of task 2 μ-tubes composition-thermal treat.	0.01	3
4	Ag nm-tubes in task 1 μ-tubes / Ag nm-tubes wall possible	0.20	16
5	Applying Ag nm-grain to task 1 μ-tubes Ag-size	0.40	16
6	Put superconformal Ag to task 1 tubes Ag. Transp dynam	0.10	16
7	Making $NiCr_2O_4$ spinel in task 2 tubes spinel size	0.10	8
8	Making Li/Ni/O spinel in task 1 tubes size-%Li	0.05	8
9	Putting Pt on task 3 tubes size, wetability NiCrN	0.08	6
10	Nafion impregnation of task 1 tubes walls pores or not	0.05	6
11	Buying polypropylene nonwoven insulation *	0	1
12	Sealing task 10 tubes bipolar separator side ends porosity	0.05	8
13	Make insulator side μ-flanges in task 13 tubes obstructions	0.03	12
14	Put chemical Ni ext part impregnated Ni tube uniform	0.05	4
15	Making a reinforced thinner plane membrane delamininate	0.30	18
16	Making carbon nanotube wall μ-tubes axial coupling	0.07	22
17	Applying Pt to task 16 tubes (used also in 19/20 tubes)*	0.02	2
18	Organometalic catalyst in task 16 tubes (8 opt) several	0.12	11
19	Nafion Impregnation of task 16/3 tubes volume controls	0.08	5
20	Sealing task 16 tubes bipolar separator side ends porosity	0.12	4
21	Making insulator side μ-flanges in task 20tubes obstructions	0.03	12
22	Applying Pt to task 21 tubes *	0.0	2
23	Applying Ru inner coat tubes task 12 or 13 tubes several	0.03	1
24	Buying 18 μm Ni foil *	0	1
25	Cr over task 24 foil *	0	2
26	Nitretation task 23 foil with Los Alamos Patent allowed?	0	2
27	Put chosen catalyst in chosen acid cathode *(if cat ok)	0	2
28	Carbon bipolar separator acquisition *	0	3
29	Integration acid cell tools/cleaning	0.03	4
30	Integration of alkaline cell tools/cleaning	0.03	4
31	Validation	0	3
-1	**Kill- no kill task**		
0	**Start / no start task**		
1	**Alkaline cathode choice**		
2	**Alkaline anode type (nafion in Ni wall or not)**		
3	**μ-flange / membrane or not alkaline mount**		
4	**Acid cathode support choice**		
5	**Acid cathode catalyst choice**		
6	**Acid anode type: NiCrN/C impreg. / membrane**		
7	**Acid mounting type**		
8	**Cell choice**		

#	Weeks	#	Weeks	#	Weeks	#	Weeks	#	Weeks
1	8	2	16	3	14	4	1	5	1
6	23	7	27	8	11	9	2	10	3

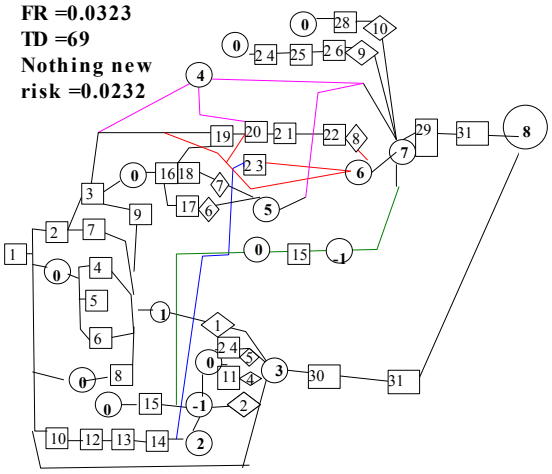

Fig. 19: Tubular Fuel Cell Task Tree.

TABLE 5: GOOD TASKS CHAIN FOR MEMBRANE COATED PEM.

#	Task / **Decision**/doubt	FR	TD
1	P_2O5^{-2}/WO_3^{-1} composite membrane	0.30	18
2	Silico-tungstic composite membrane	0.30	20
3	Perfluric ionomer cover for composite membrane	0.10	16
4	PEEK ionomer cover for composite membrane	0.40	25
5	Anodized carbon nm-tube screen	0.07	17
6	Filling with ionomer task 5 screen	0.03	3
7	Activation of task 6 part exposed carbon	0.03	3
8	Los Alamos diffuser with yarns to hold more ionomer	0.15	22
9	Alloy catalyst 1 for CH_4O /C_2H_6O	0.08	28
10	Alloy catalyst 2 for CH_4O /C_2H_6O	0.08	28
11	Alloy catalyst 3 for CH_4O /C_2H_6O	0.08	28
12	Alloy catalyst 4 for CH_4O /C_2H_6O	0.08	28
13	Platted metal bipolar separator 1	0.20	32
14	Platted metal bipolar separator 2	0.30	32
15	Platted metal bipolar separator 3	0.30	32
16	Alcohol feeding	0.03	16
17	O_2 feeding	0.03	12
18	Integration	0.03	2
19	Validation	0	3
-1	**Kill- no kill task**		
0	**Start / no start task**		
1	**Bipolar plate**		
2	**Catalyst**		
3	**Conventional new diffuser**		
4	**Membrane base material**		
5	**Membrane cover**		

#	Weeks	#	Weeks	#	Weeks	#	Weeks	#	Weeks
1	10	2	25	3	18	4	20	5	22
6	16	7	12	8					

Buying parts in the market reduces failure risks to a near null level, but these parts brings no innovation to the design. Carbon systems are intrinsically stronger but more expensive. Cleaning is the major predicted difficulty to take advantage from flow current, as if non-diffuse EBL is thicker than its 0.3 nm, its capacity decreases, and total charges also decreases.

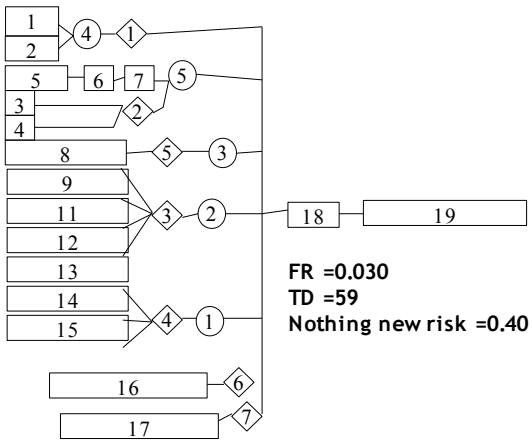

Figure 20: Good PEM Program Task Tree.

VII. CONCLUSIONS

The intensive development effort in PEM fuel cells lead some of its configurations performances very close to theoretical limits. Significant improvements in planar electrodes cells are very difficult. Jumping from gas liquid interface areas from a range of 1-10 times the nominal separators area to levels over 50, are still risky, but acceptable ones face performance increases, as shown with the Critical Chain Method. The raise in effective gas-liquid interface by unit of volume is the most important path for better performance, but effective increasing requires designs with good ionic current transport. Electrokinetic effects may have a key role in total ionic resistance, being able even to decrease them by 50%. O_2 transport improvements are mainly due to higher gas-liquid interface areas. Electrical Boundary Layer shall be better studied with other models, as the Poisson-Nerst-Planck, or models with ions size and relative positional electrostatic energy corrections. Ionic resistance is minimized with high ionic potentials and flow current near the ionic bridge boundary, where reaction rate is greater. High gas liquid interfaces dismiss the need of very effective catalysts. The joint use of better geometries and new catalysts will make fuel cells able to deliver more than 20 W/cm^3 with efficiencies over 50% in about a decade, with great impacts on the energy market.

VIII. REFERENCES

Periodicals:

[1] Antoine, O; Bultel, Y; Durand, R. "Oxygen reduction reaction kinetics and mechanism on platinum nano-particles inside Nafion". *Journal of Electroanalytical Chemistry* 499, 2001, pp. 85–94.

[2] Tromans, D. "Oxygen Solubility Modeling in Aqueous Solutions". 0-7803-5489-3/99/$10.00 01999 IEEE

[3] Ledoux, M.J; Vieira, R; Pham-Huu, C; Keller, N. "New catalytic phenomena on nanostructured (fibers and tu-bes) catalysts". *Journal of Catalysis* 216, 2003, pp. 333-342.

[4] Bambace, L.A.W; Nishimori, M; Ramos, F. M.; Bastos-Netto, D. "Performance of a double catalyst fuel cell cathode with a tubular oxygen breathing and preliminary reduction zone". Journal of Thermal Science 14(2). 2005. pp. 187-192.

[5] Bazylak, A; Sinton, D; Djilali,N. "Improved fuel utilization in microfluidic fuel cells: A computational study". *Journal of Power Sources* 143, 2005, pp. 57–66.

[6] Min, K; Tanaka, S; Esashi, M. "Fabrication of novel MEMS-based polymer electrolyte fuel cell architectures with catalytic electrodes supported on porous SiO_2". *J. Micromech. Microeng.* 16, 2006, pp. 505–511.

[7] La Coura, B.R;Schieveb, W.C. "Derivation of the Onsager principle from large deviation theory" *Physica A* 331, 2004, pp. 109 -124.

[8] Vine, S; Outhwaite, C.W. "Comparison of Theories of the Aqueous

Electric Double Layer at a Charged Plane Interface". *Biophysical Journal* 84, 2003, pp 3594–3606.

[9] Corry, B; Kuyucak, S; Chungy, S. "Dielectric Self-Energy in Poisson-Boltzmann and Poisson-Nernst-Planck Models of Ion Channels". *J.C.S.Faraday II,* 74, 1978, pp 1670-1689.

[10] Dadzie, S.K; Méolans, J. G. "Temperature jump and slip velocity calculations from an anisotropic scattering kernel". *Physica A* 358, 2005, pp. 328–346.

Books:

[11] Mitchel, W. "Fuel Cells". Academic Press. 1963.

Technical Reports:

[12] Tennison, S.R; Strelko, V; Brown, D.E; Sowerby, B. "Novel high power density carbon fibre based PEM fuel cells - Feasibility Study" MAST Carbon Ltd Report ETSU F/02/00247/00/REP. 2003

Dissertations:

[13] Easton, E.D. "Chemical Modification of Fuel Cell Catalysts and Electrochemistry of Proton Exchange Membrane Fuel Cell Electrodes", PhD Thesis. University of Newfoundland. Canada. 2003.

[14] Casey. R.J. "An Innovative Approach to Schedule Management on the F/A-22 Major Defense Acquisition Program (MDAP): Demonstration of Critical Chain Project Management". PhD thesis. Virginia University. 2005.

Patents:

[15] Bambace, L.A.W; Nishimori, M; Ramos, F. M, Melo, C.J; Kuranaga, C; Senna, J.R.S; Neri, J.A.C.F; Silva, M.D. "Conjunto capilar recirculante para células a combustível". Brazilian Patent Pending PI0301417-7. May. 2003.

[16] Ramos, F.M; Bambace, L.A.W; Melo, C.J; Nishimori, M; Kuranaga, C. "Sistema de tubos de parede eletrodepositada para células a combustível". Brazilian Patent Pending PI0301416-9. May,. 2003.

IX. Biographies

Luis Antônio Waack Bambace, was born in 18/01/1956 in São Paulo, Brazil. He graduated in Mechanical Engineering from the Escola Politécnica da Universidade de São Paulo in 1978, and get a PhD degrre in 1990 in Aerodynamics Propulsion and Energy from ITA (Brazilian Aeronautic Technological Institute). Presently Senior technologist at INPE, where develops fuel cells, satellite systems and hydroelectric subsystems. bambace@dem.inpe.br

Fernando Manuel Ramos born on 03/05/1958, in Rio de Janeiro, Brazil. He graduated from the Instituto Tecnológico da Aeronáutica-ITA, in 1981. PhD in Fluid Mechanics from École Nationale Supérieure d'Aéronautique et de l'Espace - ENSAE, France. In 1992 INPE International Relations Main Adviser, and Titular Researcher at INPE. Professor of Applied Computation Pos Graduation Program at INPE. fernando@lac.inpe.br.

Renata Favalli was born in 2/10/1971. She graduated in Mathematics from the Centro Universitário da Fundação Santo André in 1993. PhD in nuclear Science and Technology from IPEN in 2002 and Post-Doc from the Imperial College in Computational Fluid Dynamics, London in 2004. Presently working in IPEN, in fuel cells, spray dryers atomizers, plasm torches and ceramic colloids modeling. renata.favalli@gmail.com

Alfredo José Alvim de Castro was born in Rio de Janeiro, Brazil, on 13/09/1956. He graduated in Mechanical Engineering from the Pontifícia Universidade Católica do Rio de Janeiro in 1979. MSc in Mechanical Engineering from Pontifícia Universidade Católica do Rio de Janeiro in 1983, presently Senior technologist at IPEN. Experience in Nuclear Engineering and Reactor technology working mainly in: Boiling, Fluid Flow, experimental area and instrumentation. ajcastro@ipen.br

Hélcio Francisco Villanova was born in Guaratinguetá, SP, BR in 16/12/1969. He graduated in Mechanical Engineering from the Escola Federal de Engegharia de Itajubá in 1993. Get a specialization in Fluid Mechanics in INPG, France, in 1999. Msc in Space technology / Combustion in 1997, from INPE. PhD in Applied Computation from INPE in 2006, presently working with Computational Fluid Dynamics Modeling at INPE. hnova@lac.inpe.br.

PUBLICAÇÕES TÉCNICO-CIENTÍFICAS EDITADAS PELO INPE

Teses e Dissertações (TDI)

Teses e Dissertações apresentadas nos Cursos de Pós-Graduação do INPE.

Manuais Técnicos (MAN)

São publicações de caráter técnico que incluem normas, procedimentos, instruções e orientações.

Notas Técnico-Científicas (NTC)

Incluem resultados preliminares de pesquisa, descrição de equipamentos, descrição e ou documentação de programa de computador, descrição de sistemas e experimentos, apresentação de testes, dados, atlas, e documentação de projetos de engenharia.

Relatórios de Pesquisa (RPQ)

Reportam resultados ou progressos de pesquisas tanto de natureza técnica quanto científica, cujo nível seja compatível com o de uma publicação em periódico nacional ou internacional.

Propostas e Relatórios de Projetos (PRP)

São propostas de projetos técnico-científicos e relatórios de acompanhamento de projetos, atividades e convênios.

Publicações Didáticas (PUD)

Incluem apostilas, notas de aula e manuais didáticos.

Publicações Seriadas

São os seriados técnico-científicos: boletins, periódicos, anuários e anais de eventos (simpósios e congressos). Constam destas publicações o Internacional Standard Serial Number (ISSN), que é um código único e definitivo para identificação de títulos de seriados.

Programas de Computador (PDC)

São a seqüência de instruções ou códigos, expressos em uma linguagem de programação compilada ou interpretada, a ser executada por um computador para alcançar um determinado objetivo. São aceitos tanto programas fonte quanto executáveis.

Pré-publicações (PRE)

Todos os artigos publicados em periódicos, anais e como capítulos de livros.